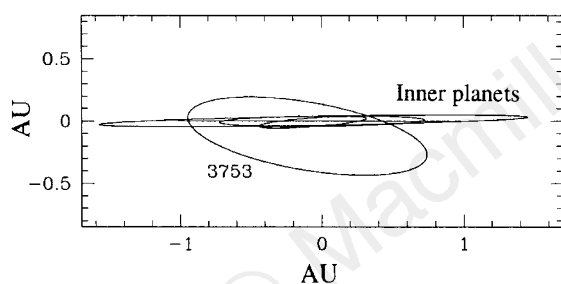


**Figure 2** The heliocentric semimajor axis  $a$  of asteroid 3753 (1986 TO) over the next 2,000 years. As the asteroid's orbital period is proportional to  $a^{3/2}$ , transitions from  $a > 1$  AU to  $a < 1$  AU or vice versa correspond to reversals of the asteroid's direction within the horseshoe.



**Figure 3** The orbits of the inner planets Mercury, Venus, Earth and Mars, along with that of asteroid 3753 when seen from the direction of the vernal equinox. The orbits of the inner planets are hard to distinguish, but the relatively high inclination of 3753 is apparent. The Sun is at the origin.

into such an unusual orbit makes a recent origin seem equally unlikely. As for the asteroid's future, though prediction is problematic owing to 3753's short chaotic timescale, a collision with the Earth seems very improbable. A strong gravitational interaction with Venus in 8,000 years seems quite likely, though the possibility of a collision with that planet at that time remains remote. On balance therefore, the origin of this object remains an enigma. More detailed investigation of this object is clearly required; even the direct exploration of 3753 by spacecraft is presumably well within the reach of current technology. □

#### Methods

The numerical simulations of asteroid 3753 presented here were performed with the Wisdom–Holman<sup>8</sup> integrator, in a model Solar System which included all the planets except Pluto. It should be noted however that the Earth–Moon barycentre was used for the Earth, an approximation which is valid because the Earth–asteroid distance is always much larger than the Earth–Moon distance. The heliocentric orbital elements of 3753 used were<sup>5</sup>: semimajor axis  $a = 0.99778030$  AU, eccentricity  $e = 0.51478431$ , inclination  $i = 19.812285^\circ$ , longitude of the ascending node  $\Omega = 126.373212^\circ$ , argument of perihelion  $\omega = 43.640637^\circ$ , and mean anomaly  $M = 40.048932^\circ$ ; these elements were calculated for epoch JD 2450500.5 and the equinox of J2000.0.

Received 10 February; accepted 1 April 1997.

1. Szebehely, V. *Theory of Orbits* (Academic, New York, 1967).
2. Dermott, S. F. & Murray, C. D. The dynamics of tadpole and horseshoe orbits. II The coorbital satellites of Saturn. *Icarus* **48**, 12–22 (1981).
3. *Minor Planet Circular 11312* (Minor Planet Center, Smithsonian Astrophys. Observ., Cambridge, MA, 1986).
4. *IAU Circ. No. 4262 and 4266* (1986).
5. Bowell, E. *The Asteroid Orbital Elements Database* available at <ftp://ftp.lowell.edu/pub/elgb/astorb.html> (1997).
6. Bowell, E. *et al.* in *Asteroids II* (eds Binzel, R. P. *et al.*) 524–556 (Univ. Arizona Press, Tucson, 1989).
7. Rabinowitz, D. L. The size distribution of earth-approaching asteroids. *Astrophys. J.* **407**, 412–427 (1993).
8. Wisdom, J. & Holman, M. Symplectic maps for the  $n$ -body problem. *Astron. J.* **102**, 2022–2029 (1991).

**Acknowledgements.** We thank M. Holman for the use of his integration codes. This work was supported in part by the Natural Sciences and Engineering Research Council of Canada.

Correspondence should be addressed to P.A.W. (e-mail: [wiegert@yorku.ca](mailto:wiegert@yorku.ca)).

## A silicon/iron-disilicide light-emitting diode operating at a wavelength of $1.5 \mu\text{m}$

D. Leong, M. Harry, K. J. Reeson & K. P. Homewood

Department of Electronic and Electrical Engineering, University of Surrey, Guildford, Surrey GU2 5XH, UK

Although silicon has long been the material of choice for most microelectronic applications, it is a poor emitter of light (a consequence of having an 'indirect' bandgap), so hampering the development of integrated silicon optoelectronic devices. This problem has motivated numerous attempts to develop silicon-based structures with good light-emission characteristics<sup>1</sup>, particularly at wavelengths ( $\sim 1.5 \mu\text{m}$ ) relevant to optical fibre communication. For example, silicon–germanium superlattice structures<sup>2</sup> can result in a material with a pseudo-direct bandgap that emits at  $\sim 1.5 \mu\text{m}$ , and doping silicon with erbium<sup>3</sup> introduces an internal optical transition having a similar emission wavelength, although neither approach has led to practical devices. In this context,  $\beta$ -iron disilicide has attracted recent interest<sup>4–12</sup> as an optically active, direct-bandgap material that might be compatible with existing silicon processing technology. Here we report the realization of a light-emitting device operating at  $1.5 \mu\text{m}$  that incorporates  $\beta$ -FeSi<sub>2</sub> into a conventional silicon bipolar junction. We argue that this result demonstrates the potential of  $\beta$ -FeSi<sub>2</sub> as an important candidate for a silicon-based optoelectronic technology.

There has been interest for some time in the semiconducting  $\beta$ -phase of iron disilicide as a possible route to optically active structures compatible with silicon technology. However, experimental investigations into this material have been limited and even its basic properties, such as the value of the bandgap energy and the type (that is, the directness), have been controversial<sup>4–12</sup>. Photoluminescence has also been observed but its origin has been disputed and has been attributed by some<sup>13,14</sup> to defects in the surrounding silicon. Recent work<sup>15,16</sup> has shown that  $\beta$ -iron disilicide,  $\beta$ -FeSi<sub>2</sub> (produced by ion implantation into device-quality (100) silicon followed by suitable annealing) is direct-gap. Photoluminescence at a wavelength of  $1.5 \mu\text{m}$  has been observed in this material and has been shown conclusively to be band-edge-related luminescence from the  $\beta$ -iron disilicide<sup>17</sup>.

Efficient semiconducting electroluminescent sources such as high-intensity light-emitting diodes (LEDs) and particularly injection lasers are made from direct-gap semiconductors, as these provide an efficient and fast radiative route. It is also necessary to incorporate heterojunctions to provide good carrier and optical

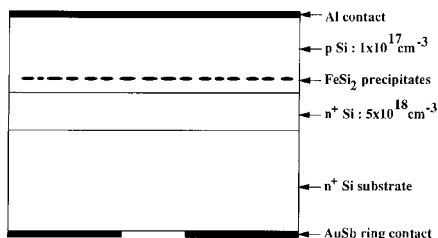
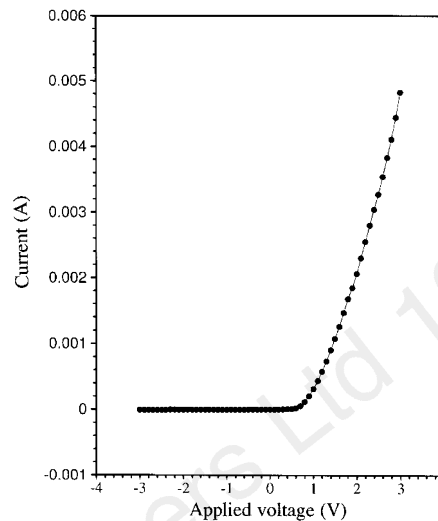


**Figure 1** Schematic of the LED structure used. Further details of the structure are provided in the text.

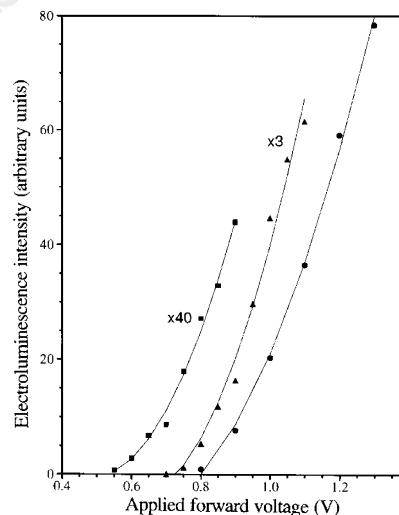
confinement and to enable efficient light extraction.  $\beta$ -FeSi<sub>2</sub> now seems to be able to offer all these properties and so this material would seem a promising route to practical optical sources in silicon. The use of ion beam synthesis to fabricate such a device is particularly attractive, as the use of many ion implantation stages is ubiquitous in the production of integrated silicon circuits, and so this technique is well suited to current silicon process technology; we note that customized implantation equipment may have to be used as was done in the case of silicon implanted with oxygen (SIMOX) technology.

We have achieved, and describe here, the successful fabrication of a demonstrator silicon/iron-disilicide light-emitting diode. The approach used is to incorporate direct-gap iron disilicide into a conventional silicon p-n junction diode, in the recombination region adjacent to one side of the depletion region, to provide a route for direct radiative recombination. Carrier injection is achieved conventionally under forward bias. A schematic of this device is shown in Fig. 1. Initially, to avoid unnecessary complications, the implantation of the iron to form the buried silicide region was made into a previously grown abrupt silicon p-n junction. The silicon p-n junction was grown by molecular beam epitaxy and consisted of a boron-doped p-type region, 1.0  $\mu\text{m}$  thick, grown on a 0.4- $\mu\text{m}$ -thick antimony doped n-type region; the doping densities in the two regions were  $1 \times 10^{17} \text{ cm}^{-3}$  and  $5 \times 10^{18} \text{ cm}^{-3}$ , respectively. These epilayers were grown on an n-type (100) silicon substrate with a resistivity of 0.008–0.02  $\Omega \text{ cm}$ . Ultimately it is anticipated that the whole device including the p-n junction could be fabricated entirely by ion implantation. The implant dose used,  $2 \times 10^{16} \text{ cm}^{-2}$ , produces isolated precipitates of single-crystal  $\beta$ -FeSi<sub>2</sub> on annealing. A continuous buried iron silicide layer can be formed if higher implant doses are used<sup>18</sup>, but we believe the use of precipitates is preferable as the implantation time and consequently the cost of device production would be reduced dramatically. Moreover, this type of structure could be realized with commercial high-current ion implanters. The precipitates are single crystal and have typical dimensions of several hundred  $\text{\AA}$ , so no quantum confinement effects are expected<sup>17</sup>. The implant energy, 950 keV, was chosen to place the peak of the precipitate distribution above the depletion region of the silicon p-n junction.

After implantation at 350 °C, the device was annealed at 900 °C for 18 hours in an optical lamp furnace in a nitrogen atmosphere, a procedure that was previously found to give good photoluminescence<sup>6</sup> but also moderate enough for diffusion of the junction dopants to be minimal; we estimate diffusion lengths for the Sb and B of  $\sim 50 \text{ nm}$ . Ohmic contacts, 1 mm in diameter, consisting of Al and AuSb eutectic were deposited by vacuum evaporation and then alloyed onto the p-type region and the n-type substrate, respectively. A window was left in the back contact to allow passage of the electroluminescence (EL) through the transparent silicon substrate. The diodes were 'isolated' by mesa etching down to the substrate material<sup>19</sup>. Current–voltage (*I*–*V*) measurements were then made to check for diode integrity. A plot of the *I*–*V* characteristic of a fully processed and working device is shown in



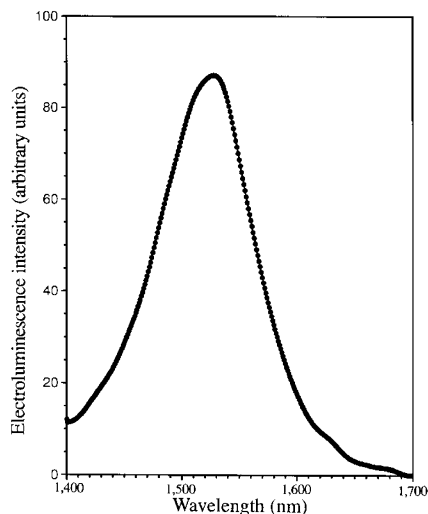
**Figure 2** The current–voltage plot for the working device measured at room temperature; the reverse leakage current is 3  $\mu\text{A}$ .



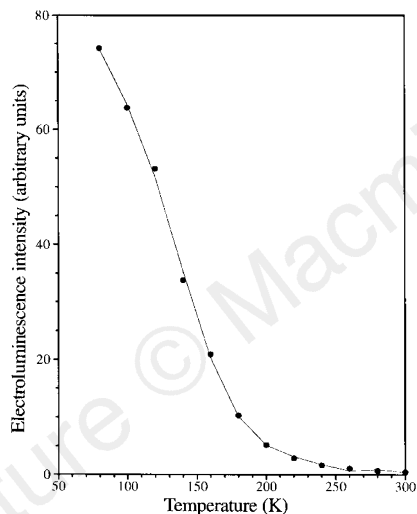
**Figure 3** Plots of the integrated electroluminescence intensity as a function of applied forward voltage at various temperatures: filled circles, 80 K; filled triangles, 180 K; and filled squares, 300 K. The solid lines are provided as guides to the eye.

Fig. 2. The good characteristics obtained demonstrate that the diode integrity has been retained throughout the device processing steps. Individual devices were separated and mounted in a variable-temperature, dynamic continuous-flow liquid nitrogen cryostat placed in front of a conventional half-metre spectrometer. A liquid nitrogen cooled germanium p-i-n diode was used for detection of the EL.

Initial EL measurements were made at 80 K. The onset of EL was seen when the diode was forward biased to around 0.8 V. The intensity of the EL emission as a function of forward bias, at various measurement temperatures, is shown in Fig. 3; the form of the curves and the values of the turn-on voltages are entirely consistent with conventional injection across the p-n junction under forward bias being the excitation mechanism. The EL spectrum taken at a forward current of 15 mA is shown in Fig. 4. The EL measured at 80 K peaks at a wavelength of 1.54  $\mu\text{m}$  and has a full width at half height of 50 meV. In Fig. 5 we show the temperature dependence of the EL intensity between 80 K and room temperature. The EL



**Figure 4** Spectrum of electroluminescence intensity against wavelength, measured at 80 K. The forward current through the device was 15 mA.



**Figure 5** A plot of the integrated intensity as a function of measurement temperature. All measurements were made at a forward current of 15 mA. The solid line is provided as a guide to the eye.

reduces with increasing temperature but could still be seen clearly at room temperature. The peak energy of the EL shifts slightly towards lower energies with increasing temperature, as expected for a band-edge-related emission. The shift in peak energy with temperature,  $\sim 50$  meV between 80 and 300 K, follows precisely that observed previously for the bandgap shift of the iron disilicide determined from an optical absorption study<sup>15</sup>.

The device was subjected to frequent temperature cycling between room temperature and 80 K; it has operated in continuous wave mode for several hundred hours. Significantly, no changes or deterioration in the EL quality, intensity or operating conditions have so far been observed.

We have demonstrated the fabrication of a working and robust LED in silicon, based on  $\beta$ -FeSi<sub>2</sub>; this LED is not just an important device in itself but is also significant as an essential first step for the subsequent development of a 1.5- $\mu$ m injection laser in silicon. The quantum efficiency of our device is low; we estimate  $\sim 0.1\%$ ,

depending on the particular operating conditions. Nevertheless, there appear to be, so far, no fundamental reasons why optimization of the device design and material quality could not lead to greatly improved efficiencies. □

Received 29 October 1996; accepted 29 April 1997.

1. Miller, D. A. Silicon sees the light. *Nature* **378**, 238 (1995).
2. Forster, M. *et al.* Photoluminescence and photocurrent studies of Si/SiGe p-i-n heterostructures. *J. Appl. Phys.* **80**, 3017–3023 (1996).
3. Zheng, B. *et al.* Room temperature sharp line luminescence at 1.5 microns from an erbium doped light emitting diode. *Appl. Phys. Lett.* **64**, 2842–2844 (1994).
4. Christensen, N. E. Electronic structure of beta-FeSi<sub>2</sub>. *Phys. Rev. B* **42**, 7148–7153 (1990).
5. Eppenga, R. Ab initio band structure calculation of the semiconductor beta-FeSi<sub>2</sub>. *J. Appl. Phys.* **68**, 3027–3029 (1990).
6. Finney, M. S. *et al.* Effects of annealing and cobalt implantation on the optical properties of beta-FeSi<sub>2</sub>. *Mater. Res. Soc. Symp. Proc.* **316**, 433–438 (1994).
7. Radermacher, K., Skeide, R., Carius, J., Klomfass, J. & Mantl, S. Electrical and optical properties of FeSi<sub>2</sub> layers. *Mater. Res. Soc. Symp. Proc.* **320**, 115–120 (1994).
8. Giannini, C., Lagomarsino, S., Scarinci, F. & Castrucci, P. Nature of the bandgap of polycrystalline beta-FeSi<sub>2</sub> films. *Phys. Rev. B* **45**, 8822–8824 (1992).
9. Rosen, B. N. E. *et al.* Characterisation of beta-FeSi<sub>2</sub>/Si heterostructures grown by gas source MBE. *Mater. Res. Soc. Symp. Proc.* **320**, 139–144 (1994).
10. Bost, M. C. & Mahan, J. E. A clarification of the index of refraction of beta iron disilicide. *J. Appl. Phys.* **64**, 2034–2037 (1988).
11. Bost, M. C. & Mahan, J. E. Optical properties of semiconducting FeSi<sub>2</sub> films. *J. Appl. Phys.* **58**, 2696–2703 (1985).
12. Dimitriadis, C. A. *et al.* Electronic properties of semiconducting FeSi<sub>2</sub> films. *J. Appl. Phys.* **68**, 1726–1734 (1990).
13. Sauer, R. *et al.* Dislocation related photoluminescence in silicon. *Appl. Phys. A* **36**, 1–13 (1985).
14. Radermacher, K., Carius, R. & Mantl, S. Optical and electrical properties of buried semiconducting beta-iron disilicide S. *Nucl. Instrum. Meth. B* **84**, 163–167 (1994).
15. Yang, Z., Homewood, K. P., Finney, M. S., Harry, M. & Reeson, K. J. Optical absorption study of ion beam synthesized polycrystalline semiconducting FeSi<sub>2</sub>. *J. Appl. Phys.* **78**, 1958–1963 (1995).
16. Katsumata, H. *et al.* Optical absorption and photoluminescence studies of beta-FeSi<sub>2</sub> prepared by heavy implantation of Fe<sup>+</sup> ions into silicon. *J. Appl. Phys.* **80**, 5995–5962 (1996).
17. Leong, D., Harry, M., Reeson, K. J. & Homewood, K. P. On the origin of the 1.5 micron luminescence in ion beam synthesized beta-FeSi<sub>2</sub>. *Appl. Phys. Lett.* **68**, 1649–1650 (1996).
18. Hunt, T. D. *et al.* Optical properties and phase transformations in alpha and beta iron disilicide layers. *Nucl. Instrum. Meth. B* **84**, 168–171 (1994).
19. Reeson, K. J. *et al.* Electrical and optical properties of ion beam synthesised (IBS) FeSi<sub>2</sub>. *J. Nucl. Instrum. Meth. B* **106**, 364–371 (1995).

**Acknowledgements.** We thank E. Parker and P. J. Phillips of the University of Warwick for growing the silicon p-n junction layers. This work was supported by the UK Engineering and Physical Sciences Research Council.

Correspondence and requests for materials should be addressed to K.P.H. or K.J.R. (e-mail: k.homewood@surrey.ac.uk; k.reeson@ee.surrey.ac.uk).

## Single-molecule optical switching of terrylene in *p*-terphenyl

F. Kulzer, S. Kummer, R. Matzke, C. Bräuchle & Th. Basché\*

*Institut für Physikalische Chemie, Universität München, Sophienstrasse 11, 80333 München, Germany*

The controlled manipulation and switching of single atoms and molecules raise the prospect of ultra-high-density data storage. Switching by motion of a single atom has been reported<sup>1</sup>, and techniques of single-molecule optical detection and spectroscopy<sup>2</sup> in the condensed phase have been refined to a degree that allows the modification of the absorption properties of a single chromophore<sup>3</sup>. Light-induced jumps in single-molecule excitation frequencies have been reported<sup>3–5</sup>, but in none of these cases could the process be controlled: the jumps varied from molecule to molecule, they were interrupted by spontaneous jumps, and the new excitation frequencies could not be identified unambiguously. Here we report light-induced reversible frequency jumps of single molecules of the aromatic hydrocarbon terrylene embedded in a particular site of a *p*-terphenyl host crystal<sup>6</sup> at temperatures of around 2 K. The changes in absorption frequency

\* Present address: Institut für Physikalische Chemie, Johannes-Gutenberg-Universität, 55099 Mainz, Germany.